

The structure of ELMs and the distribution of transient power loads in MAST

A. Kirk, R. Akers, N.J. Conway, G.F. Counsell, J. Dowling, B. Dudson 1), A. Field, F. Lott 2), H. Meyer, M. Price, M. Walsh 3), H. R. Wilson & the MAST team

EURATOM/UKAEA Fusion Association, Culham Science Centre, Abingdon, Oxon OX14 3DB, UK

1) Oxford University, Clarendon Laboratory, Parks Road, Oxford OX1 3PU, UK

2) Imperial College of Science and Technology, University of London, London SW7 2BZ, UK

3) Walsh Scientific Ltd., Culham Science Centre, Abingdon, Oxon OX14 3EB, UK

e-mail contact of main author: andrew.kirk@ukaea.org.uk

Abstract. The spatial and temporal structure of edge localised modes (ELMs) and the spatial structure of power loads during one type of disruption on MAST is presented. Filamentary enhancements of visible light are observed on photographic images of the plasma obtained during ELMs. Comparisons with simulations show that these filaments follow field lines at the outboard edge of the plasma. The toroidal mode number of these filaments has been extracted from a study of the discrete peaks observed in the ion saturation current recorded by a mid-plane reciprocating probe. A study of the time delay of these peaks with respect to the onset of the ELM has been used to calculate an effective radial velocity for the expansion of the filaments. A comparison of this derived radial velocity as a function of distance from the last closed flux surface with simulations indicates that the filament is accelerating away from the plasma. Measurements of the time difference between the peaks in the ion saturation current observed at two toroidally separated probes, when compared to these simulations, confirms this picture. A study of the toroidal velocity as a function of radius shows that during an ELM the strong velocity shear near to the edge of the plasma, normally present in H-modes, is strongly reduced. The picture that emerges is that the ELM can be viewed as being composed of filamentary structures that are generated on a 100 μ s timescale, accelerate away from the plasma edge, are extended along a field line and have a typical toroidal mode number ~ 10 . Such a structure would be expected from the theory of the non-linear evolution of ballooning modes, which also predicts filament like structures in certain types of disruptions. Evidence for these filaments as a precursor to a certain type of disruption has been obtained from both visible and infrared images.

1. Introduction

The spatial distribution of energy released from the core plasma during edge localised modes (ELMs) and disruptions is a key area of study for ITER, where the resultant power loadings, both inside and outside the divertor region, have an important impact on the choice of operating regimes and the lifetime of plasma facing materials. The excellent diagnostic views afforded by the spherical geometry of the MAST tokamak, remote first wall and extensive divertor and edge diagnostics make it an ideal device for the study of transient power loads. An important aspect of this work is the poloidal and toroidal localization of the energy deposited during the transient event and in particular the fraction that reaches the divertor compared to the first wall.

In section 2, detailed measurements of the spatial and temporal structure of ELMs observed in the MAST tokamak will be presented, which confirm a number of predictions of the non-linear ballooning mode theory [1]. This theory is also applicable to certain types of disruptions and in section 3 the evidence for the observation of filaments leading to one type of disruption will be presented.

2. The spatial and temporal evolution of ELMs

The evidence for the spatial localisation of ELM structure has come from a variety of experimental techniques [2][3]. Most striking is the unique capability on MAST to view a large fraction of the plasma surface and hence capture a picture of an ELM using a high-speed camera. Provided the exposure time is sufficiently small so that the features are not blurred, clear filaments are observed (see figure 1). In order to try to extract information on the spatial structure of ELMs from these figures, an image plane simulation for the camera has been performed [3]. Firstly, it is only possible to reproduce the number of features observed in figure 1 if the toroidal mode number (n) used is in the range 8 to 14. Secondly, the filaments appear to follow field lines with q_{95} in the range 4 to 6, however, there is some indication that the filament may twist to follow new field lines as it moves out further from the Last Closed Flux Surface (LCFS). Thirdly, it is only possible to give an upper limit of ~ 10 cm for the width of each filament as the estimate is affected by the toroidal rotation during the exposure time.

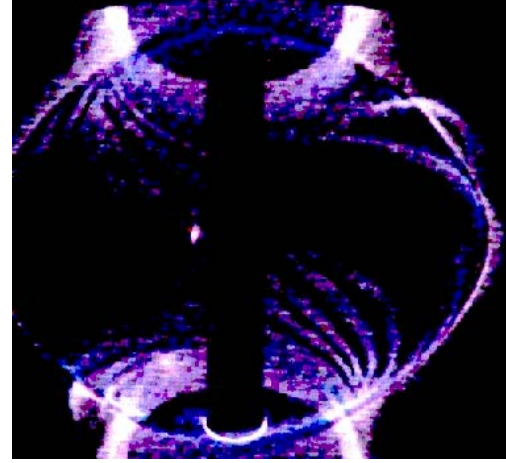


Figure 1 High-speed video image of the MAST plasma obtained at the start of an ELM.

Additional information on the toroidal localisation and radial extent of the ELM outside of the core plasma has been obtained from studies of the ion flux measured by a mid-plane reciprocating Langmuir probe [2]. The power density arriving at the probe can be considerable for distances up to 15 cm from the last closed flux surface. Figure 2 shows a plot of the ion saturation current density (J_{SAT}) observed at the reciprocating probe during an ELM and the divertor D_α where the probe was at a distance $\Delta r \sim 3$ cm from the LCFS (i.e. $\psi_N \sim 1.1$). As can be seen, during a single ELM, 3 or 4 distinct periodic peaks in the ion flux are observed. It has been found that as the toroidal velocity increases the peaks become narrower and closer together [3]. For the J_{SAT} data shown in figure 2 each peak has a full width half maximum of ~ 10 μ s and the peaks are separated by $\Delta t \sim 50$ μ s. Interpreting these peaks as filaments rotating with the plasma past the probe [2] gives a filament width in the toroidal direction of ~ 15 cm. The pitch angle of the field lines on the outboard side is $\sim 45^\circ$ implying the width of the filament perpendicular to the field lines is ~ 10 cm. This is similar to the estimates obtained from the visible images. The toroidal separation between filaments is ~ 75 cm implying a toroidal mode number of ~ 12 . The toroidal mode number has been derived for ELMs in a variety of plasmas where the probe was less than 5 cm from the plasma edge [3]. The peak in the distribution is 10 and the mean

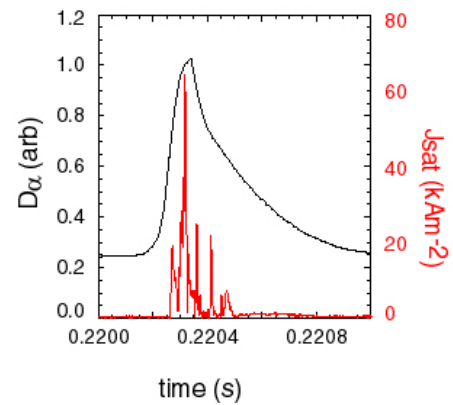


Figure 2 The D_α signal and the J_{SAT} observed at the reciprocating probe.

is 11. This is consistent with the most unstable modes typically predicted by the linear theory of ideal magneto-hydrodynamics for this range of discharges.

Normally there is a strong shear in the toroidal velocity near the edge of H-mode plasmas. In the presence of such a shear, it is difficult to see how the filament could squeeze between the field lines on neighbouring flux surfaces. The toroidal rotation has been measured at the edge of the plasma on MAST using the HELCEL diagnostic [4], which measures the radial profiles of edge toroidal impurity velocities using visible Doppler spectroscopy. The velocities are obtained at the outboard mid-plane with a spatial resolution of 5.5 mm and a time resolution of 125 μs . Figure 3 shows the toroidal velocity as a function of time relative to the peak in mid-plane D_α emission for each radial chord for a series of similar ELMs. Firstly, inside the LCFS the rotation velocity drops from $\sim 20 \text{ km s}^{-1}$ before the ELM to $\sim 12 \text{ km s}^{-1}$ at the ELM peak. The start of the change in velocity occurs effectively at the same time as the D_α light starts to rise. The chords outside the edge increase in velocity such that at the peak of the mid-plane D_α emission there is effectively no velocity shear at the edge of the plasma. The velocities return to pre-ELM values within 300 μs following the ELM.

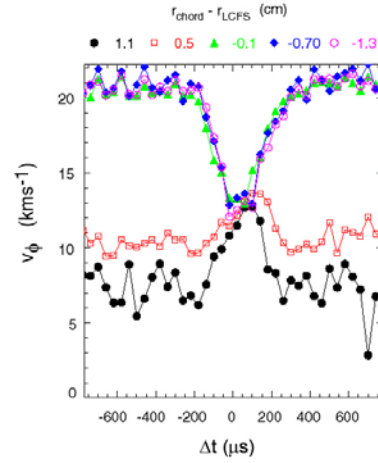


Figure 3 The toroidal velocity versus the time from the peak of the mid-plane D_α emission of each ELM for different radial chords in the edge region of the plasma for a series of similar ELMs.

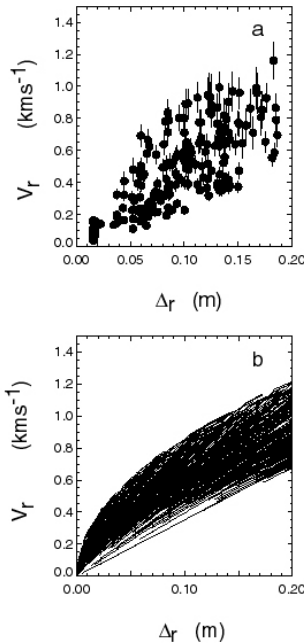


Figure 4 a) Measured and b) simulated "Radial expansion velocity" as a function of distance from the plasma edge (see text for details).

Direct measurements of the radial velocity of expansion during the ELM are difficult. On MAST it has been observed that the rise in J_{SAT} at the mid-plane reciprocating probe due to an ELM is delayed with respect to the start of the rise in mid-plane D_α emission [2]. This delay increases with Δ_r and has been used to estimate a radial expansion velocity away from the separatrix, v_r , as shown in figure 4a. A clear increase in velocity up to 20 cm from the plasma edge can be observed. In order to understand how this derived velocity is affected by the toroidal rotation of the filaments a simulation has been performed assuming that each ELM is composed of n equally spaced filaments, each having a toroidal extent of 5° at the mid-plane and rotating with a toroidal velocity of V_ϕ . One filament is generated at a random toroidal location relative to the simulated probe position and then the next $n-1$ filaments are generated at $360^\circ/n$ intervals. The experimentally observed distribution of n and V_ϕ are used. Each filament expands outwards with a radial velocity. A range of scenarios has been investigated i.e. constant velocity, constant acceleration and deceleration from an initial velocity. The time taken for

the first filament to arrive at the probe (Δt) is recorded as a function of distance (Δr) of the probe from the plasma edge. The derived radial velocity ($\Delta r/\Delta t$) is then calculated for 20 000 simulated ELMs. A comparison of the experimental data and the simulations suggest that the filament is accelerating radially outwards [3]. A good agreement with the experimental data can be obtained if the filament is made to accelerate away from the plasma with a distribution of accelerations in the range $0.5 \times 10^7 - 1.5 \times 10^7 \text{ ms}^{-2}$ (see figure 4b).

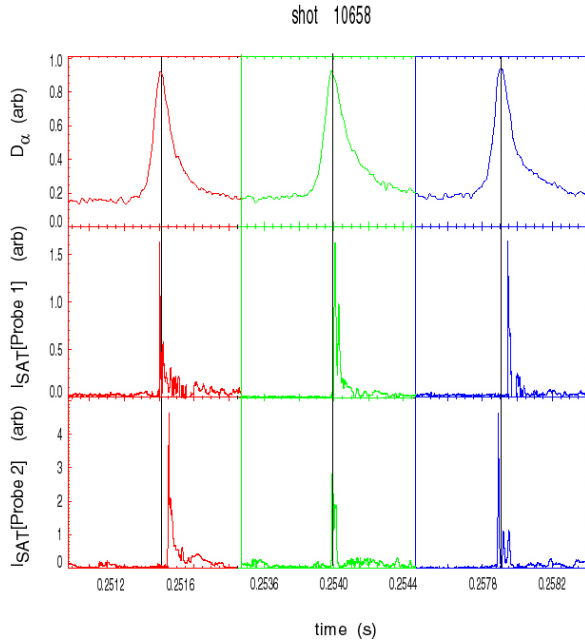


Figure 5 The D_α signal and I_{SAT} observed at the two toroidally separated probes, both at the same radial position 5cm from the plasma edge.

toroidally uniform.

Figure 6 shows the distribution of the time difference between the first peak in the ion saturation current observed at each probe for a series of ELMs. The distribution is symmetric around zero and extends to $\sim \pm 100 \mu\text{s}$. In order to determine if these data are consistent with the idea of localised toroidally rotating filaments a second probe toroidally spaced by 30° has been added to the simulation described above. The timing difference that would be observed by these two probes using the same parameters as were used for the simulation shown in figure 4b results in the solid curve shown in figure 6. As can be seen this simulation is in good agreement with the data. Hence this simulation can describe both the radial expansion and toroidal rotation of the filaments.

A second mid-plane probe has recently been installed on MAST separated toroidally from the first by 30° . Figure 5 shows the ion saturation current (I_{SAT}) recorded by the two probes for three ELMs during a single shot where both probes were at a distance of 5cm from the plasma edge. The second probe has a larger area and hence records a larger signal. The structures observed by the two probes for a given ELM are similar, however, the relative timing between the first peak is variable from one ELM to another. For the ELM at $t \sim 0.2515 \text{ s}$ the signal arrives at probe 1 first. For the ELM at $t \sim 0.254 \text{ s}$ the signals at the two probes are effectively coincident while for the ELM at $t \sim 0.258 \text{ s}$ the signal is observed first at probe 2. The fact that the timing difference changes from one ELM to another is further proof that the ELM is not

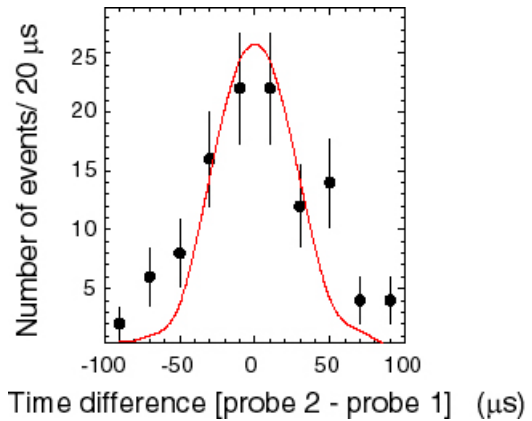


Figure 6 The distribution of time difference between the peaks in the ion saturation current at the two toroidally separated probes. The solid curve is the result of the simulation described in the text

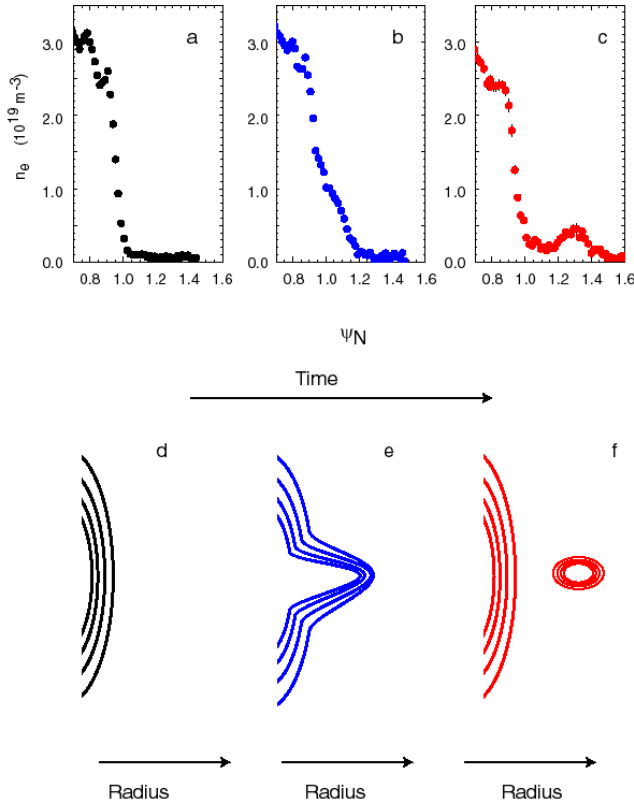


Figure 7 The time history of the effect of an ELM on the plasma.

plasma filaments would rotate with the plasma and hence would pass through the field of view of one-dimensional diagnostics. Thomson scattering measurements during this time, and for which the perturbation is in the field of view, would show the formation of a broad outboard tail (figure 7b). This disturbance to the outboard flux surfaces leads to enhanced cross-field transport of heat and particles from the filament into the scrape-off layer. Since the filament is linked to the core it acts as a conduit for losses from the whole pedestal region i.e. much more energy would be lost during the process than there is contained in the filament volume. Finally, by magnetic reconnection, the filament detaches from the core at the outboard mid-plane (figure 7f), though possibly still remaining attached to the core further along its length. Thomson scattering measurements with the correct spatial and temporal phasing now show a discrete, outboard density peak (figure 7c).

Although, the non-linear ballooning mode theory of Wilson and Cowley [1] may be able to describe the spatial and temporal evolution of the filaments it does not describe how the particles and energy released by the ELM actually leave the core. It is possible that the filament acts as a "leaky hosepipe" i.e. as the filament pushes out into the SOL it loses energy and particles from the core via cross-field diffusion. However, if during this time the filament intercepts part of the vessel then considerable power loading will occur. The amount of power arriving at the first wall compared to the divertor will depend on the distance between the separatrix and the wall, the heat flux width of the filament and the radial velocity of the filament. In MAST, due to the remoteness of the first wall, initial indications from IR thermography are that all the power released by the ELM arrives at the divertor targets [6]. However, in ASDEX Upgrade it is reported that up to 25 % of the ELM energy can be deposited on the first wall [7] and in JET it has been shown that the fraction of energy

The following is a possible interpretation of the temporal and spatial evolution of the ELM based on the images obtained and on the non-linear ballooning mode theory of Wilson and Cowley [1] and illustrated using data from the high-resolution ruby laser Thomson scattering system on MAST [5]. During the inter-ELM period steep gradients in both density and temperature develop just inside the separatrix in the pedestal region, reaching a peak shortly before the ELM (figure 7a shows a typical density profile). At this time the axisymmetric magnetic geometry would be unperturbed (figure 7d). At the onset of the ELM, narrow plasma filaments develop, locally perturbing the outboard separatrix and flux surfaces in the scrape-off layer (figure 7e). Although these are extended along a field line and thus poloidally distributed, the perturbations appear to be poloidally localised at any particular toroidal angle. These

released by an ELM arriving at the divertor decreases with decreasing gap between the LCFS and the limiters [8]. On ASDEX Upgrade evidence for a localised energy deposition has been obtained consistent with a narrow filament of plasma interacting with the limiter [7]. The radial excursion on MAST (> 20 cm) appears to be larger than that on JET (~ 10 cm) and it is important to understand the physical parameters that determine the radial excursion of the ELM. The magnetic field on MAST, especially at the outboard side, is much lower than on JET and there is preliminary evidence that shows that the magnetic field may influence the radial extent [9], although the mechanism for this is still unknown.

3. Disruption power loading

A second key aspect of transient power loading studies, where an understanding of the localisation of the energy deposited is essential, is disruptions. Several types of disruptions have been studied on MAST [10]. For example, it has been shown in reference [10] that in locked mode disruptions nearly all the plasma thermal energy can be lost from the core without any broadening of the heat flux width and due to the remoteness of the first wall effectively all of this energy arrives at the targets. However, there are other types of disruptions where this may not be the case. In particular, the non-linear ballooning mode theory proposed to explain ELMs has also been suggested as a possible explanation of disruptions in high β discharges [11]. The idea is that a low- n mode grows such that the ballooning mode threshold is exceeded locally near the plasma edge producing a radially propagating flux tube, which is connected to the core in very much the same way as the ELM. If this flux tube comes into contact with any part of any plasma facing components it could release impurities that could trigger a thermal quench.

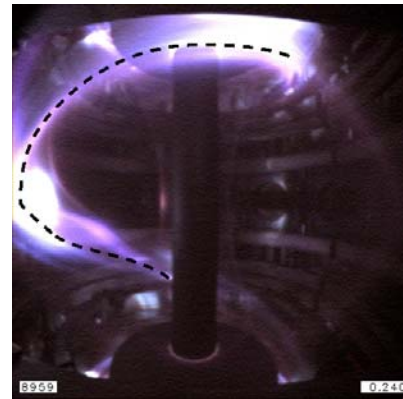


Figure 8 A high speed video image of the MAST plasma obtained just before a disruption. The black dashed line is to guide the eye.

Evidence that the ballooning mode may be responsible for such disruptions was first observed on TFTR [12] and more recently on JET [13]. The evidence for these filaments has come from the study of magnetic measurements and electron cyclotron emission (ECE) on TFTR [12] and ECE alone on JET [13]. For the first time MAST may have obtained visible and infrared images of filaments leading to disruptions. Preceding some disruptions on MAST, visible emissions are observed consistent with a single filament having an $n=1$ structure extended from the top to the bottom of the vessel (see figure 8). Recently MAST has been equipped with a fast IR camera with a wide-angle view of the entire vessel. The Poloidal Field (PF) coils are inside the vessel in MAST and are the components closest to the plasma core on the outboard side. Figure 9a shows an IR view of the vessel just before a disruption where in addition to the heat loads in the divertor, heat loads can be observed at toroidally localised positions on the top and bottom PF coils as well as near the mid-plane. It is believed that these heat loads are the result of a filament similar to that shown in figure 8. Figure 9b shows the frame obtained 3 ms later in which a plume of ablated impurities can be seen rising from one of the lower PF coils. This then 10 ms later leads to the thermal and current quench shown in figures 9c and d. The bright heat source visible at the mid-plane in figure 9d is the neutral beam dump, which is heated directly by the beam after the plasma has been

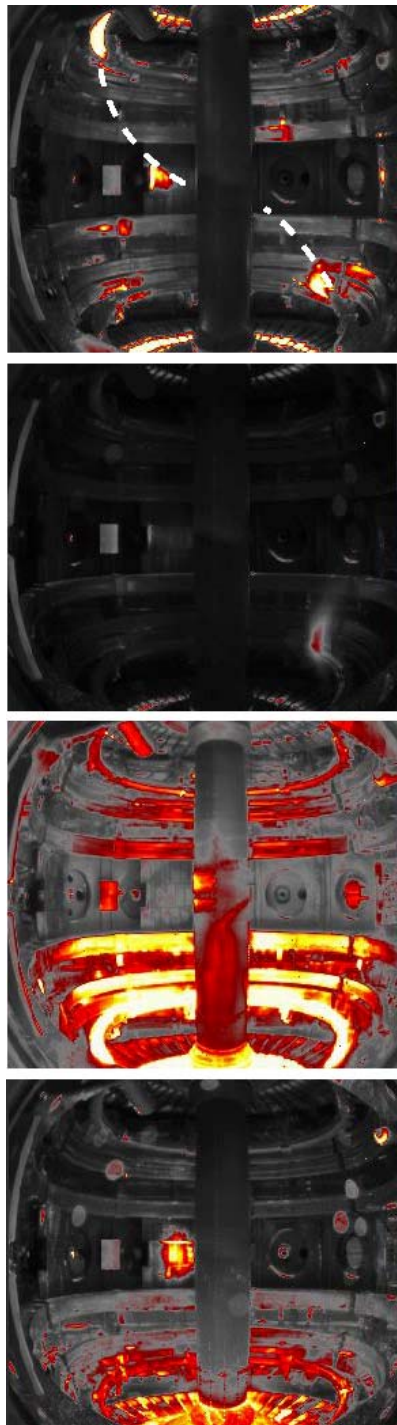


Figure 9 IR views of the plasma facing components during a disruption. The dashed line in a) represents the path of the filament (from the visible image).

a

b

c

d

extinguished. The surface temperature profiles in the divertor show a complex, evolving structure. As can be seen in figure 9d there is the formation of localised "hot-spots", possibly as a result of unipolar arc formation.

4. Summary

Measurements of the spatial and temporal structure of ELMs in MAST provide strong evidence for the ELM being a filament like structure, which is extended along a field line in such a way that at any toroidal angle it appears to be poloidally localized and at any poloidal position it appears to be toroidally localized. ELMs are measured to have a typical toroidal mode number of ~ 10 , which is similar to the most unstable modes predicted by linear ideal MHD for these plasmas. These filaments are found to expand away from the core with accelerations in the range $0.5 \times 10^7 - 1.5 \times 10^7 \text{ ms}^{-2}$. As these filaments push out from the core of the plasma there is an associated reduction in the edge velocity shear. This is a necessary condition in order to allow the filament to propagate out radially while still being attached to the core. Such a structure would be expected from the theory of the non-linear evolution of ballooning modes, adding support to the idea that peeling-ballooning modes are responsible for triggering ELM events. The theory developed and tested so far is based upon ideal magneto-hydrodynamics and therefore cannot by itself provide an explanation of the loss of heat and particles from the filamentary structure into the scrape-off layer. This theory may also be relevant to certain types of disruptions in which it predicts a low n flux tube, which would expand out rapidly and interact with vessel components leading to a thermal quench by the rapid transport of heat to these surfaces. Preceding some disruptions on MAST, visible emissions are observed consistent with a single filament having an $n=1$

structure extended from the top to the bottom of the vessel. There is also evidence that these filaments result in toroidally localised heat loads to in-vessel components.

Acknowledgements

This work was funded jointly by the United Kingdom Engineering and Physical Sciences Research Council and by EURATOM.

References

- [1] H. R. Wilson, S. C. Cowley, *Phys. Rev. Lett.* **92**, 175006 (2004).
- [2] A. Kirk *et al.*, *Phys. Rev. Lett.* **92**, 245002 (2004).
- [3] A. Kirk *et al.*, "Structure of ELMs in MAST and implications for energy deposition" submitted to *Plasma Phys. Control. Fusion*.
- [4] P.G. Carolan *et al.*, *Rev. Sci. Instr.* **72**, 881 (2001).
- [5] M. J. Walsh *et al.*, *Rev. Sci. Instrum.* **74**, 1663 (2003).
- [6] F. Lott *et al.*, "Thermographic Power Accounting In MAST " Submitted J. Nucl. Mater
- [7] A. Herrmann *et al.*, *Plasma Phys. Control. Fusion* **46**, 971 (2004).
- [8] W. Fundamenski and W. Sailer *Plasma Phys. Control. Fusion* **46**, 233 (2004).
- [9] A.Kirk *et al.*, "The spatial structure of type-I ELMs in ASDEX Upgrade" in preparation.
- [10] G. Counsell *et al.*, "Distribution of thermal energy during disruptions on MAST" Proc. 31st EPS Conf. on Plas. Phys. and Contr. Fus., (2004).
- [11] S. Cowley *et al.*, *Plasma Phys. Control. Fusion* **45**, A31 (2003).
- [12] E.D. Fredrickson *et al.*, *Phys. Plasmas* **3**, 2620 (1996).
- [13] J. Paley *et al.*, "Energy flow during disruptions in JET" Submitted to J. Nucl. Mater